Fusion enhancement for tracking of respiratory rate through intrinsic mode functions in photoplethysmography

Mikko Pirhonen and Antti Vehkaoja

Abstract –

Decline in respiratory regulation demonstrates the primary forewarning for the onset of physiological aberrations. In clinical environment, the obtrusive nature and cost of instrumentation have retarded the integration of continuous respiration monitoring for standard practice. Photoplethysmography (PPG) presents a non-invasive, optical method of assessing blood flow dynamics in peripheral vasculature. Incidentally, respiration couples as a surrogate constituent in PPG signal, justifying respiratory rate (RR) estimation. The physiological processes of respiration emerge as distinctive oscillations that are fluctuations in various parameters extracted from PPG signal. We propose a novel algorithm designed to account for intermittent diminishment of the respiration induced variabilities (RIV) by a fusion-based enhancement of wavelet synchrosqueezed spectra. We have combined the information on intrinsic mode functions (IMF) of five RIVs to enhance mutually occurring, instantaneous frequencies of the spectra. The respiration rate estimate is obtained by tracking the spectral ridges with a particle filter. We have evaluated the method with a dataset recorded from 29 young adult subjects (mean: 24.17 y, SD: 4.19 y) containing diverse, voluntary, and periodically metronome-assisted respiratory patterns. Bayesian inference on fusion-enhanced Respiration Induced Frequency Variability (RIFV) indicated MAE and RMSE of 1.764 and 3.996 BPM, respectively. The fusion approach was deemed to improve MAE and RMSE of RIFV by 0.185 BPM (95% HDI: 0.0285-0.3488, effect size: 0.548) and 0.250 BPM (95% HDI: 0.0733-0.431, effect size: 0.653), respectively, with further pronounced improvements to other RIVs. We conclude that the fusion of variability signals proves important to IMF localization in the spectral estimation of RR.

Keywords - Photoplethysmography, respiration rate, spectral fusion, synchrosqueezing, particle filtering

Corresponding Author: M. Pirhonen is with the Faculty of Medicine and Health Technology, Tampere University, Address: Korkeakoulunkatu 7 Kampusareena, 33720 Tampere, Finland (e-mail: mikko.pirhonen@tuni.fi).

A. Vehkaoja is with the Faculty of Medicine and Health Technology, Tampere University, Address: Korkeakoulunkatu 7 Kampusareena, 33720 Tampere, Finland (e-mail: antti.vehkaoja@tuni.fi).

Highlights:

- Photoplethysmographic estimation of respiratory rate by synchrosqueezing and a particle filter.
- Fusion of several respiratory-induced modulations by peak-distance correlation in spectra.
- Openly available dataset containing signals with fast variation in respiratory rates.

Unexpected changes in the respiratory response reflect a vital, primary indication for the onset of decline in patient condition, particularly of concern in clinical environment. The coupling of homeostatic feedback mechanisms to respiratory control constitutes the physiological premise for the myriad of respiratory conductors to operate on, intervening through physiological phenomena such as neural signaling, cardiac function, and biomechanical factors. The association of these respiratory-coupled mechanisms to the peripheral venous filling has been addressed in [1]. They are commonly differentiated to mechanical forces of thorax, activation of autonomous nervous system, and the bilateral signaling between these two. Among respiration-related measurands, respiratory rate (RR) is a clinically fundamental constituent in current research on physiological sensing; the monitoring of respiratory patterns proves instrumental to continuous

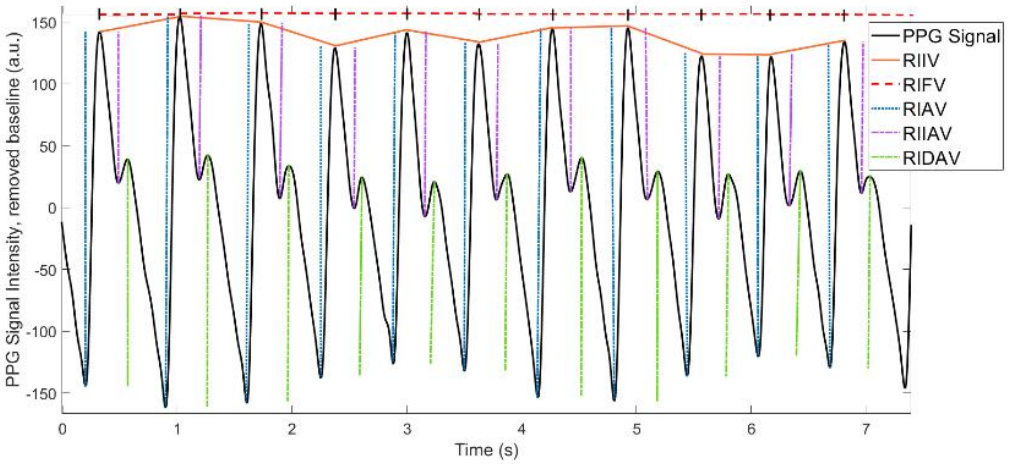

Figure 1. (Print in color) Respiratory induced variabilities, the RIVs, including both conventional and novel choices in this study. The signals stemming from these variabilities emerge from amplitude (RIAV), frequency (RIFV), baseline wander (RIIV, 'intensity'), and two formulations of amplitude distinguished at dicrotic site (RIIAV 'incisura', RIDAV, 'dicrotic').

monitoring in anesthetics, neonatal units, and surveillance of patient status e.g. through an early warning score [2]. RR acquisition may also improve the quality of patient triage (initial assessment) [3]. Due to the obtrusive nature or inaccessibility of appropriate instrumentations, the continuous respiration monitoring outside intensive care, operating theatre, or neonatal units is, however, not a part of common clinical practice. Currently, medical staff receives training on visually approximating the respiratory rate, an unsustainable effort in continuous monitoring settings and susceptible to estimation variance and human errors. Importantly, the prospects for the integration of novel RR extraction features to the clinical instrument already in widespread use, namely the pulse oximeter, implicate major convenience for clinicians. Thus, continuous RR monitoring emerges as a prospective factor in the improvement of patient safety and may prove economical to clinical environment.

Photoplethysmography (PPG) is a minimally invasive, optical measurement method, in which dynamics of subcutaneous blood flow interconnect the physiological responses to circulatory events on the periphery. Accordingly, PPG reflects parameters for both arterial and cardiac health, and the coupling of any respective surrogate events. LED photocomponents illuminate the tissue in the optical path, with the absorption of photons varying as a function of the light wavelength, the material properties of the tissue, and, importantly, the oscillating volume of blood within vasculature in cutaneous and sub-cutaneous tissue. Specifically, transmural pressure -driven motion of arteriovenous anastomosis and elasticity of cutaneous vascular plexus in dermis, as discussed in [4], induce the *apparent* increase in blood volume at the measurement site. This phenomenon is the supporting notion for reflective mode PPG while operation in transmissive mode, as in our proposed dataset, primarily accounts for the oscillations in the arterial blood supply of hypodermis. In the instrumentation perspective, the reflected or transmitted light, conditional to the applied operating mode, falls on a photodetector element, translating the blood perfusion to a distinguished pulse waveform illustrated in Fig. 1.

Significance of PPG in clinical environment has been emphasized on acquisition of heart rate (HR) and blood oxygen saturation (SpO_2) variables. Additionally, coupled with ECG, PPG proves compelling prospects for the studies of arterial health, such as atherosclerotic changes [5] or the effect of endovascular treatment [6]. Prospective monitoring sites include richly perfused areas, such as digits, wrists, brachia, and ear lobes [7]. Additionally, PPG can be measured from the forehead, yet this site may not be effective for RR estimation algorithms due to diminishment of the respiratory component relative to overall distribution of other, parasitic signal components as indicated by spectral analyses conducted in [8].

The pioneering works presented in the initial observations by Lindberg [9] and seminal review by Allen [2], and the follow-up of the scientific community, have analyzed the notion of generating the surrogate respiratory signal through morphological variations in PPG. Currently, information over respiratory components within PPG waveform has been mainly construed on evidence of variability modalities, which

are distinct mappings of an amplitude-frequency multicomponent signal. Physiologically, the signal components relate to the mechanical and nervous response of the lungs and heart through alterations in venous return and respiratory sinus arrhythmia [2]. To date, three respiratory components have been regarded as particularly important: the respiratory induced variabilities (RIV) of amplitude (RIAV), frequency (RIFV), and intensity (RIIV, also called 'baseline wander'), as discussed by [10]. These are illustrated in Fig. 1 together with two other variabilities used in the current study. Techniques for the extraction of other respiratory components, such as principal component or pulse width analysis, have been collectively discussed in [11], and are omitted here. Following algorithm phases often isolate the single most dominant component property, such as the local maxima of a time-frequency presentation, within a determined frequency region of interest (ROI) as the likely RR surrogate within these PPG-derived variability signals. However, careful considerations of the presence of parasitic components and discontinuities of respiratory components necessitates advanced methodologies to tracking of the RR estimates.

A core consideration in the construction of PPG-derived techniques lies within the limitations: due to optical recording protocol, ambient artefacts, coupled noise, and assortment of physiological regulation mechanisms, we observe the reduction of signal-to-noise ratio and masking of plausible respiratory frequencies in both data collected in controlled tests and actual operation on clinical environments. We factor major complications within PPG-RR estimates in three common notions. First, the ambient sources of error, particularly movement artefacts which introduce periodic artefact components or variation in the sensor-skin contact [12], sum into derived variability signals, invalidating prospective monitoring algorithms. Second, inter-population variability in age, gender, skin tone, and several other factors exhibit disparity translating to the morphology of PPG waveform as discussed in [2]. And third, the physiological complexity of respiration arises as a constituent of separate processes of the lungs, nervous system, and heart with fluctuating, intermittently varying contributions from each process at any single time. Regarding the last observation, the common notion in prior literature for algorithm assessment is to consider a single respiratory component at a time. However, our hypothesis is that no single RIV should be uncritically relied on during the entire RR estimation period. We estimate that the study of coherence between major spectral components for several RIV input signal permutations may assist in retaining a continuous and trackable RR component, Accordingly, the variability signal should be a fusion composite pertaining to the entire duration of respiration. This consideration for the multiparameter model has been previously discussed in [13], where the fusion through quality-controlled summation of RIV variabilities was proposed for the first time.

We have approached the evaluation of an RR estimation algorithm through the introduction of a dataset recorded on young, healthy adult subjects at sitting posture. The dataset, named 'MARSH', covers a variety of periodically metronome-assisted respiratory behavior, with each measurement lasting for 15 minutes. The core phases of our proposed algorithm include extraction of RIVs, intrinsic mode function (IMF) localization with wavelet synchrosqueezing transform (WSST), and a novel spectral fusion protocol to emphasize respiratory components. Finally, we use an iterative Bayesian tracking algorithm known as particle filter, or sequential Monte Carlo (SMC), in localizing and tracking of the instantaneous frequencies of IMFs from time-frequency representations in spectral analysis; we have based this novel approach on the support of our previous findings for its applicability with synchrosqueezing transform in RR estimation as addressed in [14]. In the study, we specified the benefits of spectral tracking as a method to extract the instantaneous frequency information by SMC with high temporal resolution.

The research questions were formulated to address both the feasibility and possible benefits of a particle filter -based tracking of a fusion spectra. The main contribution of the present study is to compare the feasibility of SMC on a variability spectrum *following* spectral fusion with conventional spectral representation lacking the fusion method. Due to nature of the tracking protocol, we study whether the proposed peak-conditioned fusion of selected RIVs appears to prevent spectral component discontinuities and enhance respiratory component from multiple input signals, thus assisting in RR component extraction. Particularly, we study these benefits conditional to different baseline RIVs, and then infer which of these RIVs provide the best baseline spectrum for the enhancement protocol. To further justify the general validity of the fusion protocol, we investigate the dominant frequencies of the spectrum directly with the reference signal, without SMC. The statistical analysis is provided by computational statistics based on Bayesian inference, discussed in [15], to answer the credibility of differences in the means of paired-sample groups: fusion and no fusion. This test has the advantage of intuitive results inference compared to traditional null hypothesis significance testing (NHST) and supersedes conventional t-testing. Furthermore, we study atypical respiration patterns and their effect on the RR estimation algorithm, and also provide an

openly available dataset applicable for such studies.

A. Related Work

Prospects for recording the surrogate coupling of RR in PPG signal have seen extensive documentation in the literature. For comprehensive reviews over the applications of PPG signal, including contexts not necessarily limited to RR estimation, the reader should refer to review articles [2], [9], and [16]. Current discussion on RR estimation algorithms includes extensive algorithm comparisons in the performance of different operational phase combinations, such as recently presented in [17]. Additionally, numerous formulations of PPG-derived respiratory signals have been proposed, such as through the use of centered-correntropy function or pulse width, and are compiled in [11].

RR estimation from respiratory components, such as RIVs, is categorizable into two domains: morphology and frequency. Latter comprise both parametric and non-parametric techniques, such as spectral and autoregressive analysis, respectively. In the morphological domain, some algorithms include heuristics, such as 'Count' methodologies proposed in [18]. Additionally, empirical mode decomposition (EMD), as proposed in [19], and its respective derivatives, have proven potentially effective in the estimation of physiological variables.

In this paper, we emphasize a technique based on the parametric, frequency domain method known as synchrosqueezing transform. The fundamental reasoning for our novel use of this approach is two-fold: respiration is a continuous variable and thus requires the extraction of the instantaneous components of signal, and the centering of the spectral power provides enhanced localization of the signal components. The rigid mathematical basis is given in [20] and the advantages and justification of the method have been realized in the authors' algorithms for RR estimation in [14]. In the latter, we have applied various derivatives of synchrosqueezing in the studies of RIAV-derived RR, for which the performance improvement to conventional spectral methods proved consistent with our hypothesis. Further support for synchrosqueezing methods has been attained by an algorithm called 'deppG', introduced in [21], where theprospects for instantaneous frequency extraction were addressed for the de-shaped synchrosqueezing transform. Extraction of IMFs from synchrosqueezed spectra should be integrated with the localization of the signal frequency of interest. Such methods could include greedy algorithms, cost functions, or Bayesian tracking.

A Bayesian localization method known as sampling importance resampling (SIR) particle filter, endorsed in the present paper, has its basis in Bayesian probability logic, and has been given the basic tutorial of formulation in [22]. Previously, particle filters have been used in RR estimation by autoregressive analysis [23]. A major advantage is the flexibility in the construction of the particle filter model. In this paper, we have opted for a simplistic structure with RR estimation by a likelihood function model, the details which are addressed briefly in this work and further in authors' prior studies on feasibility of spectral RR component extraction in [14]. One objective of this work is to address the potential of spectral fusion methods to the performance of the proposed SIR particle filter and further facilitate the prospects for IMF tracking.

Spectral fusion methods respond to the need for the fusion of the respiratory components available in PPG signals to attenuate erroneous signal transients and remove IMF discontinuities. For the respiratory component extraction, multiple component consideration, i.e. fusion phases, have been argued as a compelling consideration, an observation first studied by the signal averaging, 'smart fusion' approach in [13]. Many fusion methods have been established in the literature, such as those reviewed in [24], and share the similarity in that multiple respiratory signals are combined to provide the RR estimate. In spectral methods, previous work has been directed to averaging or cross-power multiplying of the spectrum for each respiratory signal such as presented in [25] and [26], respectively. Different time-frequency methods have been proposed for the spectral estimates, including smoothed pseudo Wigner-Ville transform with RR estimation based on the coherence of two input signals [27]. Apart from these parametric methods, other fusion techniques such as autoregressive modelling [28] or neural network evaluations [29] have been studied, these methods establishing the AR model poles or respiratory phase morphologies common for multiple input signals, respectively. In our algorithm, the most important property of a fusion method is to provide mitigation to discontinuities in instantaneous frequency ridges common to multiple respiratory signals. Contrary to other fusion methods, we formulate a mask of the commonly occurring intrinsic mode functions and sum this matrix to a spectrum from one of the RIV spectra. This gives an intuitive advantage to tracking by particle filtering in that the common IMFs are emphasized and discontinuities in single input signal spectrum are accounted for. Accordingly, we suggest a peak distance -conditioned method similar to the one proposed in [30], with differences particularly in the procedure for the summation of the spectra

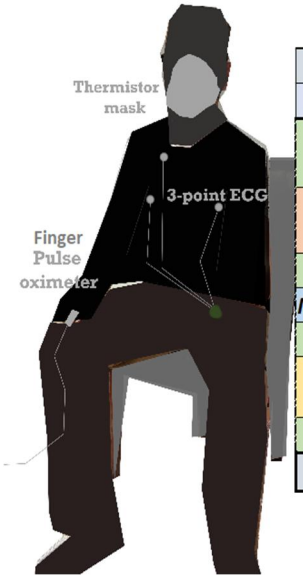

Monitoring Protocol	
Respiratory behavior	Length
Eupnea (=unlabored respiration)	3 min
Metronome, gradually increased RR (0.1→0.6 Hz)	≈ 2 min
Eupnea	2 min
Metronome, fixed 0.133 Hz	1 min
Eupnea	2 min
Metronome, gradually decreased RR (0.6→0.1 Hz)	≈ 2 min
Eupnea	3 min
Total Duration	≈ 15 min

Figure 2. (Print in color) The monitoring setup and protocol used in the data collection.

and the choice of the distance metric, coupled with a wider set of RIV signals than covered in prior literature. The purpose of the spectral fusion is to pre-condition the IMFs and as it is the particle filter output that is used to estimate the respiratory component, the fusion output is not directly meant for RR extraction as has been the case in previous studies. The proposed amalgamation of particle filtering and spectral fusion illustrates another novelty in this work. The particulars for the construction of our spectral fusion method have been addressed in the next section.

II. Materials and Methods

A. Data collection protocol and respiration patterns

The fundamental motives for the data collection involved limited amount of data available over a wide range of RR; the existing repositories often encompass merely the states of normal or exercise respiration, or the onset of a specific, medical complication such as observed in the VORTAL, CapnoBase and MIMIC-II datasets [16,31,32]. Furthermore, to provide a wide framework to conduct studies and compare several respiratory signals, we conducted a controlled protocol on healthy subjects, in which both states of eupnea and metronome-assisted respiration were replicated for the average recording duration of 15 minutes. We acknowledge the difference in the assisted and autonomic regulation of respiration. However, a metronome was deemed necessary to emulate the proposed respiratory behavior. The recorded data comprised impedance pneumography, oral-nasal thermistor, two channel ECG (Leads I and II), and PPG signal, collected from 29 subjects (ages 19 to 38, mean: 24.17 y, SD: 4.19 y, 24 males, 5 females) in sitting posture. The measurement of one subject did not include the last part of eupnea and one subject could not fully elevate the respiratory frequency. The ambient environment was controlled for minimal variations in illumination and temperature.

During the measurements, the subjects followed the protocol illustrated in Fig. 2, that includes both phases of free and metronome-assisted breathing. Ethical assessment for the recordings was provided by the ethical committee of Tampere University Hospital (R18049). We have made the annotated dataset publicly available in: (location included in the final revision of the submitted paper).

B. Algorithm construction

The structural integrity of a respiratory surrogate signal in PPG waveform reflects the variability of a weak multicomponent constituent, exhibiting slow oscillations in both, amplitude and frequency. Formally, such analytic multicomponent signal is denoted by the equation of form: $s(t) = \sum_k a_k(t) \cdot exp(i \cdot \varphi_k(t))$, where a_k and φ_k, as functions of time t, denote the amplitude and phase of the component k, respectively, and i:=sqrt(-1). Particularly, the determination of instantaneous values of the specific component is instrumental. Extracting the respiratory component from the multicomponent signal entails different

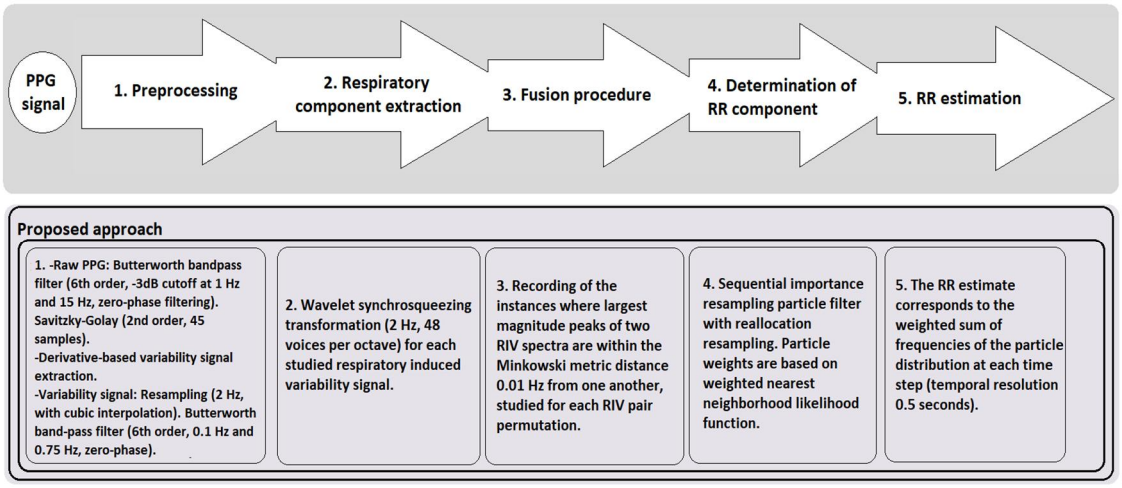

Figure 3. (Print in color) Operational phases of the proposed RR extraction algorithm.

operational phases.

As signal processing algorithms commonly consist of a series of data preprocessing and component extraction steps, each operational phase is susceptible to the attenuation of the respiratory IMF. The independency of operational phases provides flexibility, yet the performance is composed of multiple design elements, each compromising algorithm performance. Generally, operational phases include the preprocessing of the signals, the extraction of respiration component, and the determination of respiration rate. Furthermore, as stronger indication towards a combination of variability signals may prove advantageous to implement, the inclusion of a fusion phase is conceivable. The operational phases of the proposed algorithm, in their respective execution order are displayed in Fig. 3. Here, the fusion technique precedes the RR determination phase. As illustrated in Fig. 1, we have separated the three common RIVs and selected two additional variabilities, which are divisions of RIAV at the dicrotic notch (known in arterial pulse as ‘incisura’) and dicrotic peak, denoted as RIIAV, RIDAV, respectively.

Distinction over the contribution of signal magnitude and phase to RR estimate, as the separate determinants of adjacent waves, prove inconclusive due to the interwoven contribution of amplitude and frequency. The core principle in fusion methods follows the reinforcing of respiratory component IMF with methods such as inter-variability correlation, smoothening, or many-valued logic to suppress noise and IMF discontinuities. Our fusion method hypothesis is that spectral IMF ridges are reconstructible supposing that there are frequency-interval correlations of instantaneous components between the multiple comparisons of RIV variability spectra. The algorithm and figures, discussed in the following sections, were built in the MATLAB® and the R environments.

1) Signal preprocessing

Preprocessing methodologies provide the means to attenuate crude artefact and noise components. Furthermore, this phase includes the extraction of respiratory features, i.e. the points formulating each RIV signal, as they appear in the morphology of the PPG waveform. In conventional PPG analysis, the raw signal is band-pass filtered to attenuate the excess noise and low-frequency variations. The raw PPG signal in our dataset had the sampling rate of 500 Hz. Possible discontinuities are removed and interpolated here or following the ensuing RIV extraction. We have used a band-pass Butterworth filter of 6^{th} order with the -3dB cut-off frequencies of 1 Hz and 15 Hz, respectively, with zero-phase filtering. Another filter, a smoothening Savitzky-Golay of 2^{nd} order and 45 samples, was subsequently applied to the filtered signal to mitigate noise. This was followed by a first and second derivative -based morphological analysis for locating specific fiducial points in the signal as illustrated in Fig. 1 and subsequent extraction of RIV information. Extraction of RIVs was followed by resampling to 2 Hz with cubic Hermite interpolation and band-pass Butterworth filter of 6^{th} order with the -3dB cut-off frequencies of 0.1 and 0.75 Hz, in respective order.

Conventional RR estimation has been established on the grounds of PPG RIV components. The main

appeal for this approach is supported by two factors: first, the localization of the fixed points, i.e. the systolic and diastolic points, is straightforward, and second, the amplitude-frequency -connection to physiological events is preserved. Furthermore, one may distinguish additional features from the waveform, as we have shown in Fig. 1, should the arterial health of the subject make these distinctions apparent. Following this notation, one applies a suitable methodology to localize the RIV indices of interest along the PPG wave. Practical approaches, such as one applied here, characterize features based on zero-crossings of high-order derivatives. Variability terms comprise time and amplitude terms, which are interpolated to the finalized RIV signal. The following limitations should be considered; high respiration rates, exceeding half the HR frequency, are aliased as predicted by Nyquist-Shannon theorem.

2) Spectral representation of respiratory component

Signal representations in the time-frequency domain provide the basis for compelling methodologies in extraction of biophysical quantities. Parametric, spectral representations communicate the input signal segment through the convolution with a tapering function or an oscillating wavelet, which provide localization and separation of sinusoidal elements. A multicomponent signal may be decomposed in frequency components, where the IMF separation of distinct components manifests as signal ridges with slowly varying instantaneous frequencies. The main complication in the determination of IMFs is two-fold: inaccuracy in adequately fitting a non-sinusoidal, stochastic signal segment within a window function, and the cross-interaction in closely localized IMFs prompting spectral leakage and smearing artefacts, respectively.

Wavelet synchrosqueezing transform (WSST) is a nonlinear time-frequency representation (TFR) methodology to suppress the spectral leakage by reassignment of signal component energies. The kinetics 'squeezes' IMFs towards their centroids, effectively circumventing the Heisenberg-Gabor limit, the constricting factor for spectral resolution denoted by the limit $\Delta f \Delta t \geq 4\pi$ [33]. The core idea in WSST entails the detection of oscillatory components through minor shifts in the signal frame, differentiating components on mathematical separation conditions, and reassigning energy at instantaneous frequency. The mathematical details of WSST have been discussed in [21]. For this study, the scaling of the analytic Morlet -type mother wavelet was parametrized to 48 voices per octave with a sampling rate of 2 Hz. Differentiating intrinsic components along the TFR necessitates a choice on a localization algorithm. Whereas consensus states that the greatest magnitude component approximates the most relevant constituent in ROI, the lack of guarantee for continuous signal ridge suggests one to implement mathematical, penalty-thriven logic to follow IMFs. The respiratory component is presumed to be the largest component in the ROI.

3) Particle filtering

Greedy algorithms, Bayesian tracking, and cost functions may provide means to approach the localization task in IMF extraction. We have applied the SMC particle filtering method, where one iterates prior knowledge of the observations to successive steps, or states, and updates the posterior knowledge according to likelihood functions and discretized distribution dynamics. Here the posterior densities characterize spectral IMFs. The advantages of the method include managing ill-behaved transients and relatively simple evaluation. Some limitations arise due to *a priori* considerations in the likelihood function for particle weight evaluation and suppressed particle kinetics for sequential MCs during fast-changing RR.

SMC, or particle filtering, draws a state vector at successive data points, entailing information on a discretized probability density distribution and process noise. Each data point in the vector represents a particle, a constituent characterized by localization in frequency, time, and probabilistic weight. Altogether, the expectation value of the state vector, by a quantitative measure such as weight-adjusted mean, indicates the localization target of the input segment. The proposed algorithm is designed as a conventional sampling importance resampling (SIR) filter, an SMC method to recursively update the state vector. Each state is generated as follows: sample points are drawn from a distribution comprised of prior and process noise, latter approximated here as Gaussian $N(0,5e^{-3})$.

In this paper, we have applied the weighted nearest neighbor likelihood function previously proposed in [23], originally derived for the autoregressive model analysis of the RR estimate, and given as

$$w^i(n) = exp\left(-\frac{\left(R^i(n) - p^a_{nn(i)}\right)^2}{2\sigma^2_{gau}}\right) * exp\left(-\frac{\left(p^m_{nn(i)} - p^a_{max}\right)^2}{2\sigma^2_w}\right) / \left(\Sigma^{Kroi}_{m=1} * exp\left(-\frac{\left(p^m_{nn(i)} - p^a_{max}\right)^2}{2\sigma^2_w}\right)\right), \quad \textbf{(1)}$$

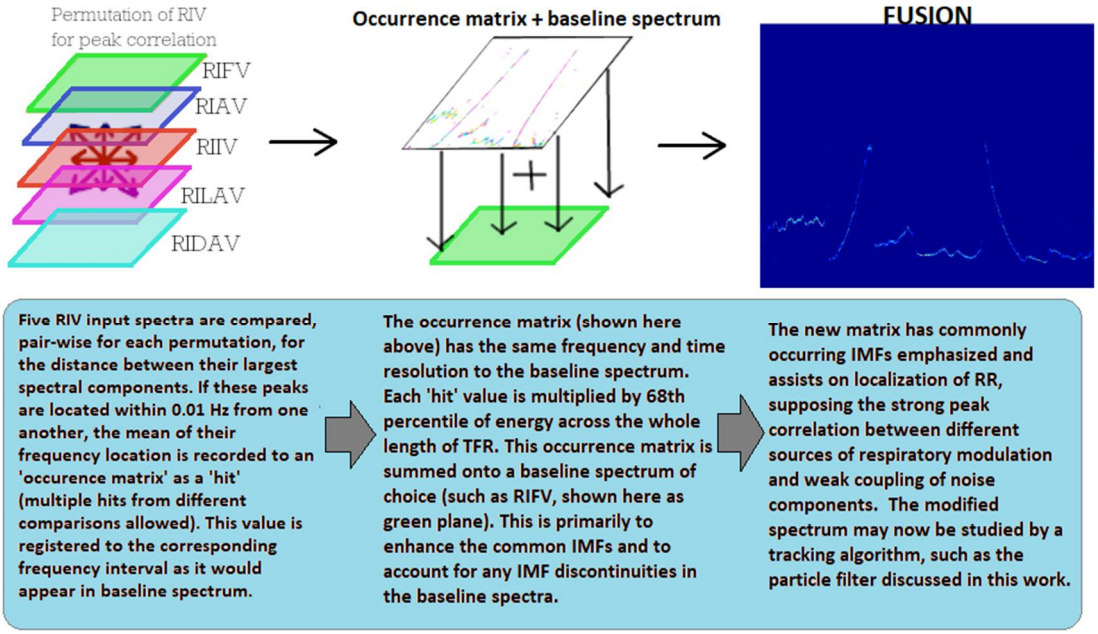

Figure 4. (Print in color) Principle of the proposed fusion method. The permutation of baseline spectra provides the occurrence matrix for fusion of components.

where we have chosen the following parameters to be used: $\sigma_{gen} = 5*10^{-3}$, $\sigma_{gau} = 5*10^{-3}$, $\sigma_{w} = 1*10^{-3}$, the number of largest components evaluated $K_{roi} = 1$. $R^{i}(n)$ represent particle location, p^{a}_{max} is the component angle with the largest magnitude, p^{a}_{nn} and p^{m}_{nn} are the nearest frequency and magnitude to the particle, respectively, computed separately for each particle for likelihood weight which together then formulate the posterior probability distribution. Following the evaluation in (1), the estimation of RR occurs by the weighted sum of frequencies in the particle population. Resampling constitutes the removal of particles with negligible weights (below 1/N, where N is the number of particles, here N = 100) and regenerating the particle number by introducing new particles conditional to a specific reallocation resampling criterion for the next iteration. Rationale for resampling is two-fold: the particles with negligible weight do not contribute to the extraction of the tracked component, yet increase relative computational expense, and neglecting the generation of new particles would eventually diverge to the evaluation of a single particle, latter phenomenon known as particle degeneracy. We have applied the reallocation resampling scheme, discussed further in [15] and [34]. In short, this resampling scheme preserves particles above the weight of 1/N and, for the next state, split into integer multiplier of particles according to their prior weight. At the beginning of the next cycle, additional particles are introduced to prior particle distribution to preserve the total number of particles. Gaussian noise jitter, here a zero-mean process noise with variance $\sigma_{gen,}$ is added before each successive reallocation step to prevent degeneracies in the filter behavior.

C. Spectral fusion

A fundamental deficiency within RR estimation in the RIV signals manifests through variability in physiological behavior during respiration, conditional to a degree with the individual health. As we have previously stated, the activity of lungs, heart, and the complex neural signaling, provide the surrogate action over the fluctuations of each RIV. Accordingly, we propose a simplistic fusion mechanism in synchrosqueezing environment formed by five RIV signals. Relevant steps leading to this peak distance - conditionalized fusion have been illustrated in Fig. 4 together with a brief description of the technique, for which the strict details are given in the next paragraph.

Initially, we extract five separate WSST representations, one for each RIV signal, retaining each TFR as equisized matrices of time-frequency bins. Following this, we estimate a Minkowski metric, Euclidean distance, for the separation of WSST ridges for each permutation pair of five matrices. In each permutation, we study the distances between the largest magnitude peaks. The algorithm is set to retain the distance information conditional to a threshold value. Here, we have used a threshold value of 0.01 Hz (0.6 BPM).

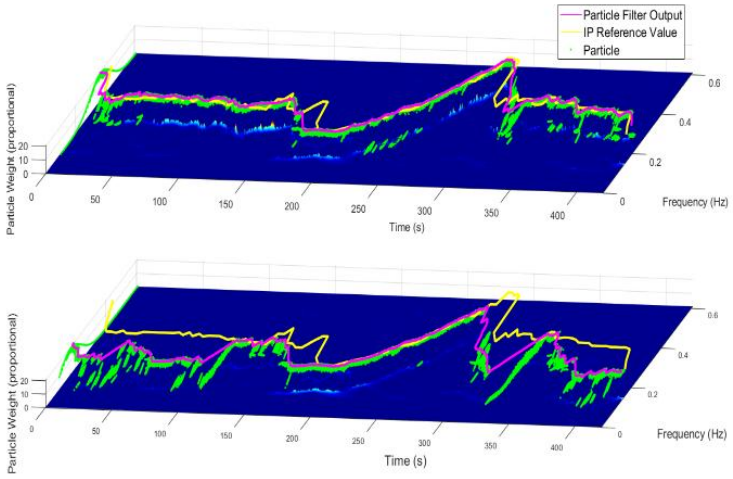

Figure 5. (Print in color) Improvement of the spectral tracking by the proposed fusion method. Fusion method (top) enhances both TFR accuracy and particle filter performance over a single RIV variable, RIAV in this example (bottom).

This threshold value was selected based on preliminary observations on similarly occurring IMFs. Consequently, we construct a matrix according to the number of times the peaks occurred within this distance for each permutation. Should the same frequency interval include a 'hit' in more than one permutation, the matrix index is summed for that frequency bin for each occurrence. The localization of the 'hits' within the matrix is the frequency point closest to average frequency between the two peaks. The appropriate magnitude of spectral energy for the occurrences is estimated according to approximate baseline energy across a RIV spectra of choice: the fusion occurrence matrix is multiplied based on a value determined from the entire baseline RIV spectrum energy, forming a separate fusion spectrum. This spectrum is summed with the baseline RIV spectrum that was used for the determination of spectral energy, to provide a new, mask-enhanced TFR. In the Results section, we have considered fusion on each RIV separately. If we determine the SIR equation only conditional to the largest spectral magnitude, the fusion emphasizes a single ridge, attenuating parasitic ridges and predicting a continuous path for the localization of instantaneous frequencies. Importantly, the permutation study by the fusion method may alleviate the discontinuities in the baseline spectrum. The improvement of spectral fusion over no fusion is shown in Fig. 5, where RIAV is considered. Here, one can visually distinguish a plausible performance improvement following the introduction of the fusion method.

The fusion estimate matrix has the *a priori* execution variables as follows: the maximal peak Euclidean distance between two RIV spectral ridges d = 0.01 Hz, the RIV baseline energy measure as the 68^{th} percentile of energy across the whole length of TFR, and the sampling rate of 2 Hz. We note that the performance of the fusion method is always conditional to at least two RIVs at any single iteration, hence the algorithm operates to combine information not from a single RIV signal to another baseline RIV but rather from a correlation in each RIV pair. This way, we are assured that a RIV with substantially different spectral composition or energy does not mask the performance of other RIVs and that crude transients from any single RIV do not translate over. As we will later observe, the fusion estimate matrix summed on top of the most potential RIVs in terms of RR acquisition does not explicitly mean equal improvement in performance for each RIV due to difference in baseline spectral energy and the baseline quality.

D. Statistical Analysis

Regarding our statistical analysis, we apply Bayesian inference (not to be confused with particle filtering), in addition to conventional statistical measures. In this paper, we have applied the statistical library BEST, presented in [15] as an alternative method superseding the traditional t-test. We have used the R environment for the Bayesian testing. The Bayesian inference method allows us to make intuitive observations from differences between two groups of results, differing with respect to whether the fusion method was applied or not. In this respect, we may omit the ambiguity of p-value discussion and represent our intervals of confidence with flexibility. Statistical variables include the difference of group means (pair-

wise test), 95% high-density credible intervals, and the effect size. The effect size, by which we refer to Cohen's d -value, is a sample size -independent measure over the magnitude of the effect on an intervention. It is calculated by difference between two group means over their pooled standard deviation. Value of 0.2 indicates a small effect while a value larger than 0.8 implies a large effect of intervention [35].

Performance evaluation of the proposed method was done based on conventional measures of statistical dispersion and population mean difference analysis, including effect size calculation. The statistical metrics introduced in the results included mean absolute error of the whole protocol (MAE) and portions of free breathing (MAE-FB), median error, and root-mean square (RMS) error. In the proposed analysis, respiration rate extracted from the IP signal was used as the reference and was found to have good correlation with RR based on oral-nasal data. We applied a conventional peak detection algorithm to calculate the respiration cycle lengths from the end points of inspiratory phase in IP signal. Prior the peak detection, the IP signal was detrended and a Savitzky-Golay smoothing filter (2^{nd} order, 91 samples, sampling rate of IP signal was 250 Hz) was applied to raw signal, which was then studied in intervals of 1.5 seconds. We proceeded to manually correct any missing or incorrectly labelled peaks. Furthermore, the study-specific measures comprised percentual proportions of measurement error, here the MAE, falling below 2 breaths per minute (BPM), denoted as coverage probability (CP_2), with the definition originally formulated in [36]. In addition, we propose hypothetical analysis based on either one or five greatest magnitude peaks on the spectra and determine the error from the closest peak to reference. While the 5-peak measure is intractable in practice, we may indicate whether the spectral fusion improved the spectral ridges regardless the effect of particle filtering.

Computational Bayesian inference provides advantages over the frequentist logic (e.g. NHST). It alleviates ambiguity surrounding hypothesis testing in p-value analysis, such as p-hacking by modifying experimental setup, and yielding intuitive information over the intervals which one expects the data distribution to credibly occupy. Essentially, Bayesian and frequentist inference answer the same questions over data through different interpretation; the Bayesian approach fixes the data and will permit the sampling distribution to evolve, whereas vice versa is observed by frequentist means,. Further, as computational tools have become more effective, the field of statistical analysis has been gradually leaning over to Bayesian methods. Thus, we will apply the Bayesian test for the difference of population group mean, corresponding to paired-sample t-test in frequentist perspective, to reflect the possible advantage observed by spectral fusion before and after the fusion technique. The technique comprises a Gibbs sampler in MCMC framework provided by BEST library. Furthermore, we will present the effect size for all results. Here, we would expect the MAE to be approximately normally distributed. A noncommittal prior was used for the Bayesian analysis.

III. Results

The evaluation of the results has been partitioned as follows: the robust statistics have been disclosed in Table 1, including the results gained by the fusion method, their SD, and the benefit acquired by fusion in WSST TF representations, in respective order. The baseline spectrum for the fusion has been specified in the columns separately for all RIV signals. For RIVs other than RIFV the results reflected clear improvement, while for RIFV the fusion method proved only modest changes. The 95% Highest Density Interval (HDI) represents the interval 95% of the results are expected to occupy. If HDI includes a range with different signs, one should not make any far-fetched assumptions on the measure, because this means that we do not have 95% credibility, which we assume noteworthy, over change due to intervention. For RIFV, we may expect the MAE, RMSE, and MAX5 to improve by introducing the fusion method, with median, MAE during eupnea (MAE-FB), CP_2, and MAX1 showing possible indications for improvement, but statistically inconclusive. From MAE-FB values, we observe that fusion method is feasible even during apnea, albeit less so than for the entire measurement duration. For other RIVs, the improvement is apparent to all proposed measures, and often accompanied with notable change. Incidentally, we observed a notable peculiarity of superior performance for RIIV at higher RRs, notably those over 0.4 Hz. While the improvement does not translate well to overall results, this finding could have important consequences to the performance of fusion algorithms.

Descriptive statistics include the Bland-Altman –type mean-difference plot given in Fig. 6, including customary 1.96σ Limits of Agreement (LOA) -statistics indicating interval of approximately 95% of the observed values. In this figure, we illustrate the mean-difference plot for fusion enhanced RIFV in a circular form, incorporating further information by a histogram representation for the distribution of the observed

reference RR frequencies and MAE in a form of a heatmap for discrete frequency intervals, in respective

Table I The fusion algorithm performance as indicated by commonly disclosed measures. SD is given in the parenthesis. Improvement due to the fusion method is given in brackets.

Method → Error ↓	RIFV	RIAV	RIIV	RIDAV	RIIAV
-MAE (BPM)	1.764 (0.6595) [-0.185]	2.0356 (0.6506) [-0.606]	2.4375 (1.0190) [-0.465]	2.1114 (0.7380) [-0.727]	2.0275 (0.6792) [-1.237]
-MAE-FB (BPM)	1.1314 (0.8793) [-0.0849]	1.2920 (0.7462) [-0.502]	1.9124 (1.1719) [-0.365]	1.3794 (0.8159) [-0.327]	1.3374 (0.7612) [-1.113]
-RMS (BPM)	3.996 (1.0963) [-0.250]	4.1874 (0.9776) [-0.538]	4.2928 (1.1191) [-0.396]	4.1913 (1.0175) [-0.565]	4.0935 (0.9404) [-1.020]
-CP2 (Breaths %)	81.119 (10.29%) [2.802]	76.1222 (13.44%) [10.25]	68.6038 (22.32%) [9.012]	74.2398 (15.45%) [7.50]	75.6318 (13.38%) [22.10]
-MAX1 (BPM)	2.2140 (0.8160) [-0.087]	2.6760 (1.0080) [-0.7362]	3.1680 (1.3920) [-0.8940]	2.6640 (1.0860) [-0.612]	2.4150 (1.2180) [-1.896]

order towards the center of the figure. Accordingly, the circular outlay connects in a practical manner multiple sources of information. The heatmap in the innermost circle indicates the direction of error at specific reference RR intervals, red color indicating frequency intervals with major impact on error value, while the change from yellow to green indicates lowering MAE contribution. In essence, this heatmap indicates the difficulty for the particle filter to assess the major transient from the end and start of the first and last metronome-emulated respiration states. From the histogram, drawn using the reference RR, the reader can observe the usual respiratory frequencies, noting that this distribution peaks at 8 BPM, corresponding to the respective, metronome-emulated state. In the mean-difference plot of the outermost circle, difficulties in the distinction of multiple points were overcome by a density representation, provided by the means of Voronoi Tessellation point density representation. We observe both crude outliers, which we denote as occurring due to difficulties in the localization of metronome-assisted respiration response,

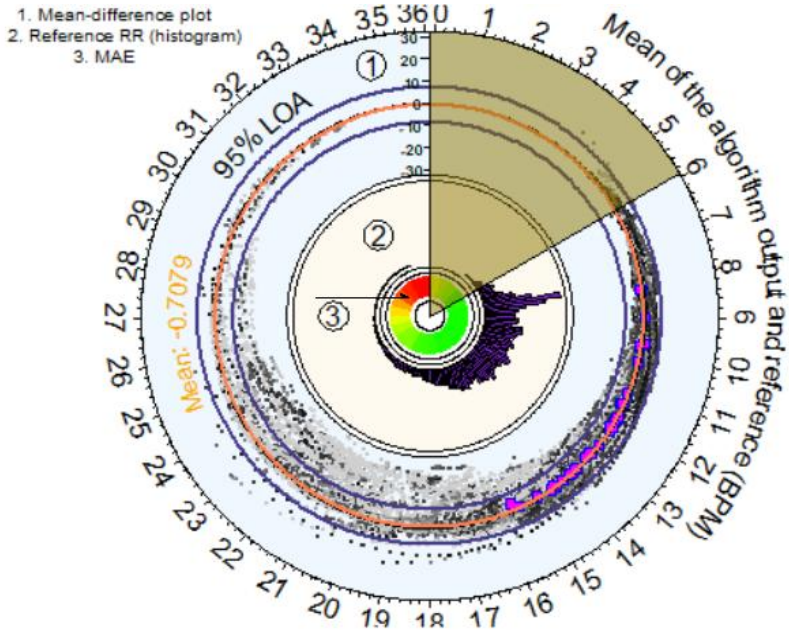

Figure 6. (Print in color) Mean-difference plot for the fusion-enhanced RIFV output. The sector in dark yellow is not part of ROI. Points in pink represent mean values of individual subjects. Point densities illustrated by Voronoi Tessellation -estimate.

yet also agreement with the reference RR, particularly at lower frequencies typical for normal, unlabored breathing. The mean values for each individual subject have been shown by pink points. The mean and 1.96σ LOA were observed at -0.7079 BPM, and [-8.071, 6.655] BPM, with $\alpha = 0.05$ confidence intervals of LOA as [-10.4461, -5.6959] BPM and [4.2802, 9.0304] BPM. Similar results have been observed previously in [9], yet due to the nature of the measurements, the outliers in this data were particularly distinctive and these particularly accentuated the magnitude of RMS error. We conclude that while there are crude outliers, they are sparse in number, and especially during unlabored respiration, the results appear to have a good correlation with the reference.

Fig. 7 illustrates the Bayesian 95% credible intervals and the effect size for each RIV and their respective statistical measures, colored with respect to the specific RIV and the statistical measure. The circular layout with its information further completes the presentation in Table 1. The figure is read from the baseline RIV, following the color-coded arrow to the error measure of interest. These values indicate the difference between fusion and non-fusion groups in the respective error measures, a negative value indicating improvement with fusion, except for the CP_2 value for which an increase is preferable. We observe varying levels of performance improvements produced by the fusion method, with each arrowhead pointing towards the mean of the 95% credible interval, shown as colored strips of the respective baseline RIV. At the base, the reader may evaluate the effect size, color-coded for each error measure, which indicates a large effect of intervention (effect size > 0.8) for most improvements. The most notable exception is the small effect size 0.113 for RIFV with respect to change in median error between fusion and non-fusion groups, also shown uncertain according to its 95% credible interval.

IV. Discussion

The results acquired from the comparisons between fusion and non-fusion groups provide several insights

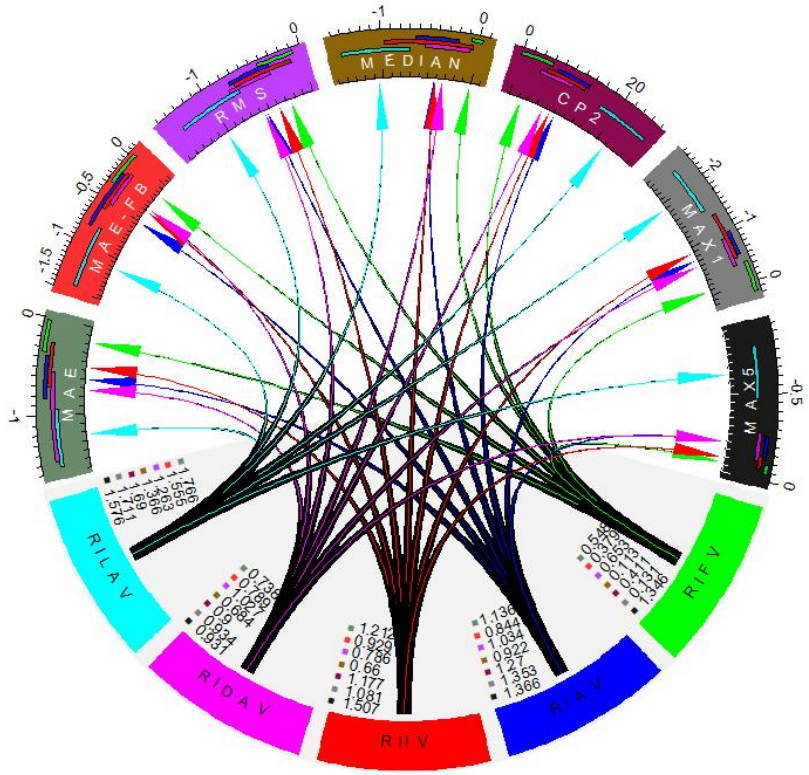

Figure 7. (Print in color) Visual depiction of the effect of the fusion method on the results. The figure shows the difference in means of various error measures between fusion and non-fusion groups (arrowhead) for paired Bayesian t-test, their credible intervals (95%, colored strips), and the effect sizes (arrow root, unitless), for the five RIVs. Results in BPM except for CP_2 (percentual change). Connection between RIVs and error measures are color-coded according to their respective color scheme.

to the research questions. First, we observe that there is a credible improvement provided by the fusion method and thus in the tracking performance of particle filtering. RIFV provided the best baseline component for the proposed algorithm in this dataset with MAE of 1.76 BPM and 1.13 BPM for eupnea (MAE-FB). The fusion benefits indicate that peak-distance relation of IMFs in multiple RIVs provides important improvement for tracking protocol, with benefits in MAE ranging from 0.19 to 1.24 BPM and 0.08 to 1.11 BPM for MAE-FB as indicated by Table 1. Furthermore, the MAX1 results indicate that respiratory component is readily available on all proposed RIV spectra. However, it would appear that the current algorithm does not perform well in fast changes in high respiratory rates, and this may be due to the simple configuration of the particle filter, which defines the trade-off between fast response and stability of the output. Additionally, the high quality of RIFV-derived RR component meant that fusion benefits for this baseline signal were not major. Larger effect is expected in older, especially elderly, subjects who generally have attenuated respiratory sinus arrhythmia.

A few important notes should be made from Table I. First, choosing the maximal peak as the RR component (MAX1) performs inferior than the MAE obtained by particle filtering even though we observed that the particle filtering performed subpar during fast changes of respiration rate in metronome-assisted phases. Clearly, fusion benefited the lower quality RIVs proportionally more than RIFV, these showing consistent improvement on all accounts. In any case, fusion was seen to improve the results with either minor or marked magnitude, and as shown in the Fig. 7, the effect sizes following the fusion method indicate a sizeable effect of intervention. Deterioration of results due to the fusion algorithm was not observed in any circumstances according to 95% HDI, although in few instances the benefits remained statistically inconclusive such as in the comparison of difference of median error between fusion and non-fusion RIFV groups. High RR frequencies proved rather challenging and the innermost circle in Fig. 6, representing MAE at specific reference RR, further indicates the difficulty in establishing high RR with appreciable accuracy on this relatively challenging dataset.

Both high respiration frequencies and transient-like changes in respiratory patterns provided major difficulty for particle filtering. This challenge was highlighted in the present study due to the test protocol used. While the performance was deemed somewhat compelling at lower frequencies of eupnea, the metronome-assisted respirations at non-fixed frequencies were difficult to distinguish, either due to aliasing in situations where the heart rate was less than twice the respiration rate or due to the fixed parametrization of an SIR filter. We believe that specialized particle filter designs, such as those implementing forward-backward iterations, could provide improvement over simple SIR filter design. Even though the results compare to previous findings for RR estimation, the nature of respiration variation in this dataset challenges most of the RR algorithms. We associate the crude outliers in the mean-difference plot to the elevated and depressed metronome-assisted phases. For a retrospective comparison without the fusion method, results obtained by our spectral particle filter algorithm in VORTAL dataset, proved slightly less compelling for RIAV, with MAE, median, and RMSE of 2.33, 1.15, and 3.68 BPM, respectively [11], while for this study the corresponding results for RIAV were 2.64, 1.1, and 4.72 BPM, respectively. However, for this paper, the crude outliers of the challenging respiratory behavior clearly affected the results, particularly the sensitive RMSE value. The portions of eupnea (RIAV-FB) indicated MAE of 1.79 BPM (without fusion), and as such indicate the potential of our dataset for further studies. In the VORTAL dataset, the respiration is mostly stationary, and thus no direct comparison of results is justifiable.

V. Conclusions

We have proposed a simple framework for an SIR particle filter algorithm with the fusion of PPG-derived respiratory variabilities in wavelet synchrosqueezing environment, and provided a new dataset, comprised of healthy, young adult subjects, for further research and evaluation of algorithms. Our main findings indicate that frequency variability of the transmissive mode PPG signal, RIFV, provides the most compelling baseline signal in the spectral analysis of RR components, and that peak-conditionalized fusion of this variability signal with other PPG-derived variabilities provides an improvement to RR estimation when coupled with particle filtering. Additionally, we observed distinct and credible improvement in RR estimation with each of the other studied RIV input signals used as the baseline. We associate these benefits with the proposed fusion process mitigating discontinuities and emphasizing the ridges of the tracked spectral IMFs. The peak-conditioned fusion method provides an intuitive way to enhance a RIV baseline spectrum by studying the commonly occurring spectral energies between different RIV spectra and translating similarities in the largest magnitude spectral components over to a baseline spectrum of choice. The results show distinct benefits to our previous studies on RR component tracking and to blind spectral

component estimation (i.e., MAX1). While the RR during the states of eupnea was accurately estimated, we also observed a few limitations with the algorithm performance. The SIR filter proves sub-optimal for large transients and there were limitations due to *a priori* heuristics in the parametrization, necessitating further research.

The findings fortify the notion that improvement in particle filter performance, and thus RR estimation, is achievable with fusion methods and that multiple RIVs hold respiratory information that should be combined to improve algorithm performance. Particularly, the localization of spectral IMFs appeared to improve following the introduction of fusion methodology, and this improvement was also translated to particle filtering performance. Furthermore, the strong agreement of WSST with the reference IP signal, in presence of challenging RR dynamics, indicates that the dataset, which has been made available in the electrical appendix of this paper (in final revision), provides an adequate basis for further studies.

Acknowledgements: This study was partially funded by the Academy of Finland (grant number 292477).
Conflict of Interest: The authors declare no conflict of interest.

REFERENCES

1. Meredith, David J., et al. "Photoplethysmographic derivation of respiratory rate: a review of relevant physiology." *Journal of medical engineering & technology* 36.1 (2012): 1-7. DOI:10.3109/03091902.2011.638965
2. Allen, John. "Photoplethysmography and its application in clinical physiological measurement." *Physiological measurement* 28.3 (2007): R1. DOI:10.1088/0967-3334/28/3/R01
3. Shah, Syed Ahmar, et al. "Respiratory rate estimation during triage of children in hospitals." *Journal of medical engineering & technology* 39.8 (2015): 514-524. DOI:10.3109/03091902.2015.1105316
4. Kamshilin, Alexei A., et al. "A new look at the essence of the imaging photoplethysmography." *Scientific reports* 5 (2015): 10494. DOI:10.1038/srep10494
5. Peltokangas, Mikko, et al. "Areas under peripheral pulse waves: a potential marker of atherosclerotic changes." *Physiological measurement* 39.2 (2018): 025003. DOI:10.1088/1361-6579/aaa46b
6. Peltokangas, Mikko, et al. "Effects of percutaneous transluminal angioplasty of superficial femoral artery on photoplethysmographic pulse transit times." *IEEE Journal of biomedical and health informatics* 23.3 (2018): 1058-1065. DOI:10.1109/JBHI.2018.2851388
7. Tamura, Toshiyo, et al. "Wearable photoplethysmographic sensors—past and present." *Electronics* 3.2 (2014): 282-302. DOI:10.3390/electronics3020282
8. Hernando, Alberto, et al. "Finger and forehead PPG signal comparison for respiratory rate estimation based on pulse amplitude variability." *2017 25th European Signal Processing Conference (EUSIPCO)*. IEEE, 2017. DOI:10.23919/EUSIPCO.2017.8081575
9. Lindberg, Lars-Göran., et al. "Monitoring of respiratory and heart rates using a fibre-optic sensor." *Medical and biological engineering and computing* 30.5 (1992): 533-537. DOI:10.1007/bf02457833
10. Li, Jin, et al. "Comparison of respiratory-induced variations in photoplethysmographic signals." *Physiological measurement* 31.3 (2010): 415. DOI:10.1088/0967-3334/31/3/009
11. Charlton, Peter H., et al. "An assessment of algorithms to estimate respiratory rate from the electrocardiogram and photoplethysmogram." *Physiological measurement* 37.4 (2016): 610. DOI:10.1088/0967-3334/37/4/610
12. Wijshoff, Ralph WCGR, et al. "Reduction of periodic motion artifacts in photoplethysmography." *IEEE Transactions on biomedical engineering* 64.1 (2016): 196-207. DOI:10.1109/TBME.2016.2553060
13. Karlen, Walter, et al. "Multiparameter respiratory rate estimation from the photoplethysmogram." *IEEE Transactions on biomedical engineering* 60.7 (2013): 1946-1953. DOI:10.1109/TBME.2013.2246160
14. Pirhonen, Mikko, et al. "Acquiring respiration rate from photoplethysmographic signal by recursive bayesian tracking of intrinsic modes in time-frequency spectra." *Sensors* 18.6 (2018): 1693. DOI:10.3390/s18061693
15. Kruschke, John "Bayesian estimation supersedes the t test." *Journal of experimental psychology: General* 142.2 (2013): 573. DOI:10.1037/a0029146
16. Charlton, Peter, et al. "Breathing rate estimation from the electrocardiogram and photoplethysmogram: A review." *IEEE Reviews in biomedical engineering* 11 (2017): 2-20. DOI:10.1109/RBME.2017.2763681
17. Charlton, Peter, et al. "Extraction of respiratory signals from the electrocardiogram and photoplethysmogram: technical and physiological determinants." *Physiological measurement* 38.5 (2017): 669. DOI:10.1088/1361-6579/aa670e
18. Schäfer, Axel, and Karl Kratky. "Estimation of breathing rate from respiratory sinus arrhythmia: comparison of various methods." *Annals of biomedical engineering* 36.3 (2008): 476. DOI:10.1007/s10439-007-9428-1
19. Madhav, Venu, et al. "Estimation of respiration rate from ECG, BP and PPG signals using empirical mode decomposition." *2011 IEEE International instrumentation and measurement technology conference*. IEEE, 2011. DOI:10.1109/IMTC.2011.5944249
20. Daubechies, Ingrid, et al. "Synchrosqueezed wavelet transforms: An empirical mode decomposition-like tool." *Applied and computational harmonic analysis* 30.2 (2011): 243-261. DOI:10.1016/j.acha.2010.08.002
21. Cicone, Antonio, and Hau-Tieng Wu. "How nonlinear-type time-frequency analysis can help in sensing instantaneous heart rate and instantaneous respiratory rate from photoplethysmography in a reliable way." *Frontiers in physiology* 8 (2017): 701. DOI:10.3389/fphys.2017.00701

22. Arulampalam, M. Sanjeev, et al. "A tutorial on particle filters for online nonlinear/non-Gaussian Bayesian tracking." *IEEE Transactions on signal processing* 50.2 (2002): 174-188. DOI:10.1109/78.978374
23. Lee, Jinseok, and Ki H. Chon. "An autoregressive model-based particle filtering algorithms for extraction of respiratory rates as high as 90 breaths per minute from pulse oximeter." *IEEE Transactions on biomedical engineering* 57.9 (2010): 2158-2167. DOI:10.1109/TBME.2010.2051330
24. Charlton, Peter, et al. "Breathing rate estimation from the electrocardiogram and photoplethysmogram: A review." *IEEE reviews in biomedical engineering* 11 (2017): 2-20. DOI: 10.1109/RBME.2017.2763681
25. Lázaro, Jesús, et al. "Deriving respiration from the pulse photoplethysmographic signal." *2011 Computing in Cardiology*. IEEE, 2011. Available: http://ieeexplore.ieee.org/document/6164665/
26. Leanderson, S., et al. "Estimation of the respiratory frequency using spatial information in the VCG." *Medical engineering & physics* 25.6 (2003): 501-507. DOI: 10.1016/S1350-4533(03)00017-1
27. Orini, Michele, et al. "Estimation of spontaneous respiratory rate from photoplethysmography by cross time-frequency analysis." *2011 Computing in Cardiology*. IEEE, 2011. Available: https://ieeexplore.ieee.org/abstract/document/6164652
28. Madhav, K. Venu, et al. "Extraction of respiratory activity from ECG and PPG signals using vector autoregressive model." *2012 IEEE international symposium on medical measurements and applications proceedings*. IEEE, 2012. DOI: 10.1109/MeMeA.2012.6226650
29. Johansson, Anders. "Neural network for photoplethysmographic respiratory rate monitoring." *Medical and Biological Engineering and Computing* 41.3 (2003): 242-248. DOI: 10.1007/BF02348427
30. Dehkordi, Parastoo, et al. "Extracting instantaneous respiratory rate from multiple photoplethysmogram respiratory-induced variations." *Frontiers in physiology* 9 (2018). DOI:10.3389/fphys.2018.00948
31. Karlen, Walter, et al. "CapnoBase: Signal database and tools to collect, share and annotate respiratory signals." *2010 Annual meeting of the society for technology in anesthesia*. Society for technology in anesthesia, 2010.DOI:-
32. Johnson, Alistair, et al. "MIMIC-III, a freely accessible critical care database." *Scientific data* 3 (2016): 160035. DOI:10.1038/sdata.2016.35
33. Poisson, Oliver, et al. "New signal processing tools applied to power quality analysis." *IEEE transactions on power delivery* 14.2 (1999): 561-566. DOI:10.1109/61.754104
34. Li, Tiancheng, et al. "Resampling methods for particle filtering: classification, implementation, and strategies." *IEEE Signal processing magazine* 32.3 (2015): 70-86. DOI:10.1109/MSP.2014.2330626
35. Sawilowsky, Shlomo. "New effect size rules of thumb." *Journal of modern applied statistical methods* 8.2 (2009): 26. DOI:10.22237/jmasm/1257035100
36. Barnhart, Huiman X., et al. "An overview on assessing agreement with continuous measurements." *Journal of biopharmaceutical statistics* 17.4 (2007): 529-569. DOI: 10.1080/10543400701376480